Laboratory study and measurement of stiffness and compaction of unsaturated clay soil by using the innovative rebound hammer

Estudio de laboratorio y medición de la rigidez y compactación de suelos arcillosos insaturados mediante el uso del innovador martillo de rebote

Behrouz Halimi[1], Hamidreza Saba [2*], Saeid Jafari MehrAbadi[1], Saeid Saeidi Jam[3]

[1]Department Of Engineering , Arak Branch, Islamic Azad University, Arak, Iran.
[2]Department Of Civil Engineering, Tafresh University, Tafresh , Iran.
[3]Department Of Civil Engineering , Hamedan Branch, Islamic Azad University, Hamedan, Iran.

* hr.saba@aut.ac.ir

ABSTRACT

Defining soil behavioral parameters, which eventually results in predicting every short-term and long-term soil behavior, has continually been one of the interests of soil mechanics and has been of exceptional value. To this end, in this study, a novel method has been reviewed to determine the compressive behavior of fine-grained soils in the laboratory and the field, without sampling by the patented electronic device. In the lab, homogeneous materials of the intended soil underwent the compaction test, mechanical and physical tests, direct shear test, and impacts of the innovative rebound hammer in the horizontal and vertical directions in the test-box. The impact shear waves produce resistance and voltage output by force and dislocation sensors with high-sensitivity proportional to the pressure based on the soil surface stiffness. The obtained voltages are then converted to digital by an analog-to-digital converter and a microcontroller. Next, a number is shown on display by the "CodeVision" program. Then, by solving a quasi-dynamic equation (Viscoelastic spring-damper model) by MATLAB software and with the aid of laboratory-field results and correlation equations, a fitting connection between all effective mechanical soil parameters has been estimated to an acceptable extent. The effective mechanical parameters of the soil include the compaction percentage, specific gravity, and frequency of the system in the damped and non-damped states, the energy imposed on the soil, and the plastic stage strain in the range of less than 15% humidity. The results determine that increased hammering numbers are directly related to increased soil compaction and stiffness. In more detail, the reading of hammer numbers less than 2 corresponds to compaction of less than 75%, while the reading of hammer numbers greater than 3 in the vertical and 2.94 in the horizontal directions on clay surfaces designates compaction of 90%.

Keywords: rebound Hammer, compressive behavior, soil stiffness, spring-damper model, unsaturated clay

RESUMEN

La definición de parámetros de comportamiento del suelo, que eventualmente resulta en predecir cada comportamiento del suelo a corto y largo plazo, ha sido continuamente uno de los intereses de la mecánica del suelo y ha sido de un valor excepcional. Para ello, en este estudio se ha revisado un método novedoso para determinar el comportamiento compresivo de suelos de grano fino en el laboratorio y en el campo, sin muestreo por el dispositivo electrónico patentado. En el laboratorio, materiales homogéneos del suelo previsto se sometieron a la prueba de compactación, pruebas mecánicas y físicas, prueba de cizallamiento directo e impactos del innovador martillo de rebote en las direcciones horizontal y vertical en la caja de prueba. Las ondas de corte de impacto producen resistencia y salida de voltaje mediante sensores de fuerza y dislocación con alta sensibilidad proporcional a la presión basada en la rigidez de la superficie del suelo. Los voltajes obtenidos se convierten luego a digitales mediante un convertidor de analógico a digital y un microcontrolador. A continuación, el programa "CodeVision" muestra un número en la pantalla. Luego, al resolver una ecuación cuasi-dinámica (modelo viscoelástico de resorte-amortiguador) mediante el software MATLAB y con la ayuda de resultados de campo de laboratorio y ecuaciones de correlación, se ha estimado una conexión adecuada entre todos los parámetros mecánicos efectivos del suelo en un grado aceptable. Los parámetros mecánicos efectivos del suelo incluyen el porcentaje de compactación, la gravedad específica y la frecuencia del sistema en los estados humedecido y no humedecido, la energía impuesta al suelo y la deformación de la etapa plástica en el rango de menos del 15% de humedad. . Los resultados determinan que el aumento del número de martilleos está directamente relacionado con una mayor compactación y rigidez del suelo. Más detalladamente, la lectura de números de martillos menores a 2 corresponde a una compactación menor al 75%, mientras que la lectura de números de martillos mayores a 3 en la dirección vertical y 2.94 en las direcciones horizontales en superficies de arcilla designa una compactación del 90%.

Palabras clave: Martillo de rebote, comportamiento compresivo, rigidez del suelo, modelo resorte-amortiguador, arcilla insaturada

1. INTRODUCCIÓN

In soil engineering, several soil behavioral parameters are achieved throughout laboratory or field operations. In this regard, the somewhat time-consuming conduction of the experiments, their expense, and the demand for expertise and accuracy to accomplish satisfactory results, has always been more or less a concern (Aflaki, I, 2008). Soil behavioral parameters ultimately result in obtaining the soil bearing capacity, determining the dimensions of foundation, stability control of the gables, investigation, and control of slip and possible rupture of ruptured wedges, determining the dimensions of the foundation and controlling the settlement, and predicting all short-term and long-term soil behaviors. In general, obtaining soil behavioral parameters, including elastic modulus, specific gravity, compaction percentage, stiffness, energy imposed on the soil, and others, depends on the accurate determination of the stated parameters. Among the physical parameters and properties of different soil types, compressibility and stiffness are critical discussable matters.

On the other hand, the soil compaction and its impact on the primary characteristics of the soil, including settlement and permeability, are essential. Furthermore, the study of soil compaction

rate is not independent of the study of specific weight changes and porosity together with changes in moisture percentage (Ashmawy, A. K, 1995). In 2014, researchers at Shahrekord University were able to make a comparison of the horizontal and angled permeability meter (PR) measurements on the interaction of silty clay soils in vitro and the presentation site, using the three-dimensional finite element method. Using the behavioral model (Drucker-Prager), they were able to estimate soil resistance parameters, including Poisson's ratio, moisture percentage, bulk compaction, Young's modulus, single-axis pressure, and other soil plasticity parameters. Additionally, in 2014, Swiss researchers compared parameters like the Poisson's ratio, present vertical stresses, elastic modulus, specific gravity, and other practical coefficients regarding the elastic behavior of the soil, using the Boussinesq's stress distribution method at a 30 to 70cm depth through numerical analysis and field studies, employing the method of transferring vertical stresses by agricultural machine tires in situ (Dos, Brajaw, 2008).

In 2016, a method was proposed by Australian scientists to determine the compressive strength of decaying materials (e.g. collapsing soil) based on measurements of the in situ shear wave velocity. In the control conditions, the deterioration degree of such deposits was studied. After analysis, the injection was performed by adding cement for cementing the deteriorating zones. At the end of the study, the percentage of added cement for optimal mixing was obtained 20% (Eflaki, Ismail, 1989). In this research, by designing a novel electronic device with high sensitivity and accuracy, the stiffness and unsaturated clay compaction factors have been examined. The study aims to discover a new approach to determine the compressive behavior of fine-grained soils in the laboratory and the field, without sampling with the patented electronic device. However, in this paper, with the help of this device as a paired method along with other conventional and new methods, by tapping on the soil surface, the parameters of their mechanical behavior are determined. Non-destructive tests were done with high repetition and with exact laboratory and field controls and different percentages of compactness by the portable light machine in field and laboratory conditions. The processed results of employing the blow of a special hammer with high sensitivity to a 13cm depth of soil were recorded in the screen of the device. Using these results, the behavioral parameters of the fine-grained soil are controlled.

 After mathematical analysis of mechanical-electrical models ("equivalent circuit") in the main memory, this device can monitor the output values derived from the mechanical properties of the desired surfaces, including stiffness, specific gravity, compaction percentage, and other requisite parameters prompted by Electric pressure created by the impact for the operator. The general objectives of the research and the purpose of inventing the rebound hammer: (A) Decreasing the costs of geotechnical and field studies in the laboratory and field, (B) Determining the mechanical behavior parameters in high-sensitivity unsaturated clay soils, (C) Diminishing the human and device errors to learn the practical parameters in the laboratory and field, (D) Improving the precision of the output results of soil resistance factors by employing soil mechanics and electronic systems and sensors (NDT non-destructive tests) in electronic science, (E) Defining and measuring pivotal parameters in soil dynamic and static loads, such as soil cohesion, compaction percentage, specific gravity, stiffness, energy imposed on the soil and moisture percentage at different levels and with higher accuracy and sensitivity than in theoretical and empirical relationships. (F) Use of shear wave theory, before and after damping in unsaturated clay and g) performing non-destructive testing on the soil surface without sampling with engineering judgment. Also, one of the most significant benefits of the invented rebound hammer device is the ability to be carried and its lightness (weighing around one-kilogram).

2. MATERIALS AND METHODS

2-1. Structure of the rebound hammer device (patented machine) and analysis of results, using the CodeVision software.

The operative characteristics of the device involve the following five general parts (Figures 1 and 2):

(A) Impact detection sensor (Hanumantha Rao, B, & Taradutta Panda, 2014)
(B) Electrical signal amplifier and filter
(C) Central Processing Unit (CPU) (Iranian Schools' Renovation Organization, 2016)
(D) The output unit (monitoring LCD)
(E) Power supply
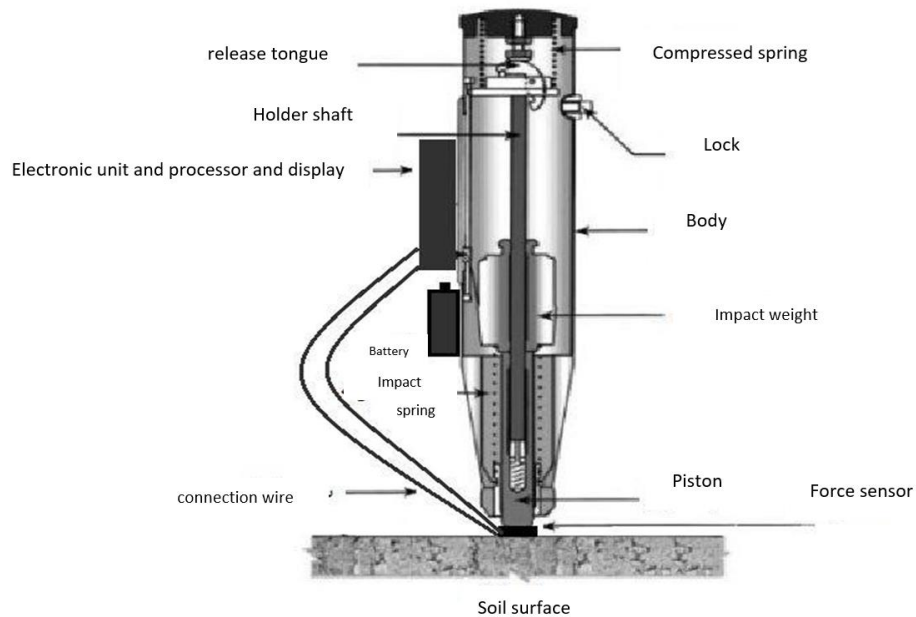
Figure 1. Schematic illustration of the hammer device with internal belongings

Figure 2. The testing of Electronic rebound hammer device

2-1-1. The device's operation

713

At first, the impact detection sensor converts the hammer tip impact to the soil surface into an analog electrical signal. Also, to eliminate noise and distortions, as well as to amplify it, the input signal enters an op-amp layer and then a filter layer. Then, when the signal is available for processing, it is carried to the central processing unit (CPU). There, under the programming pre-saved in the device's processor (CodeVision program), using the acceleration-time Figure, and the integration of the surface under the velocity and distance curves, the elastic and plastic states of the soil affected by the stiffness reflection of soil surfaces previously written in the digital logic language and related programming language, the input information is processed. The output is then presented graphically and numerically on the system monitor.

2-1-2. Calibration and correlation of the rebound hammer device with the direct shear test machine

In this step, the results of the output of the system in various stages, and different types of clay soils in terms of compaction, stiffness, and moisture, are tested in the direct shear machine and compared with the output of the electronic device and calibrated. Next, a direct relationship between the hammer number and clay is obtained in terms of stiffness and compaction percentage, which will be the basis of the research (Keller, Thomas, M & et al ,2014), (Kramer, S. 2009).

2-1-3. Simultaneous analysis of the results of the outputs of the rebound hammer and direct shear machine, and analysis of impact before and after application to the soil in the spring-damper model (validation of results)

In this step, all the output results of the rebound hammer, the direct shear machine of the laboratory, the mathematical analysis of the quasi-dynamic equation of the impact before and after reaching the soil surface are calibrated together by MATLAB software. Considering the available literature and logical theoretical relationships and hand-operated calculations, practical tables were prepared to learn the behavioral parameters of clay soils with various compaction conditions (Law, K.H, 2014), (Lin, J., Y, 2014) and (Moore, D.M, 1989).

2-2. Preparation of optimal homogeneous materials for research and laboratory tests.

The clay of the study was selected. Then, initial tests were done on specific gravity, compaction, compaction percentage, XRD, plastic limits, granulation, and direct and single-axis shear. By knowing the type and characteristics of the studied clay, the practical parameters are compared with the fabricated device (Naderi-Boldaji, Mojtaba, et al, 2014).

2-3. Determination and analysis of specific gravity and the soil compaction percentage

Soil compaction test (modified Aashto-C method) was performed on parametric samples in the range of 1.18 to 1.89gr/cm3 and the compaction percentage in the range of 71.95% to 100% in the laboratory on the desired clay (Moore, D.M, 1989).

Then, tests on soil surfaces were performed on 17 parametric samples by the rebound hammer device. Finally, given the specific gravity and percentage of the available compaction s, the

hammer numbers of the device are read at every stage of the test and listed in the results tables. Using the correlation relationships and graphs obtained, an accurate interpretation of the link between hammer numbers and specific gravity and homogeneous clay compaction is readily provided in the conclusion section.

2-3-1. Soil compaction test (ASAASHTO T 180 - 70 & ASTM D 1557 - 70)

The modified AASHTO-C method was employed to determine the specific gravity under some moisture and compaction conditions. The altered hammer is like standard ones. Water was added to each soil sample to reach the desired moisture content. The five layers of soil were changed using a modified automatic hammer and compacted according to AASHTO T180 (ASTM D 1557) in a standard four-inch mold. The T180 method works a 10-pound hammer with a drop distance of 18 inches, generating a 356,000 ft-lbf/ft force. Hammer behavior and falling distance increase with compaction. The earlier standards have been issued by the American Highway and Transportation Association, 444 North Capitol Street, Suite 249, Washington DC, 2001 (Figure 3) (Moore, D.M, 1989). The results determine that the maximum dry unit weight of clay in the optimum moisture is 15.63%, which is equal to 1.64 g/cm, and its maximum wet unit weight is 1.90 g/cm. Ultimately, at least 136 tests were performed on soil samples with specific gravity and moisture conditions in the laboratory (Table 1), (Figure 3).

Table 1. Soil compaction test

| Mold weight: 2400 g - Mold size: 81/665 cm^3 - C Method								
Sample number	1st	2nd	3rd	4th	5th	6th	7th	8th
Mold and soil weight (gr)	470	4850	4910	5060	5150	5235	5223	5190
Wet unit weight (gr/cm^3)	1.35	1.50	1.56	1.72	1.81	1.90	1.89	1.85
weight of the container, and wet sample (gr)	59.30	59.50	48.50	80.00	53.50	91.80	89.40	45.70
weight of the container, and dry sample (gr)	58.50	57.50	46.30	75.00	49.00	83.80	80.40	40.40
Sampling container weight (gr)	21.4	21.4	15.7	28.6	14.4	30.4	30.4	13.5
Moisture percentage (%)	2.15	5.54	7.19	10.7	13.0	15.6	18.0	19.7
dry unit weight (gr/cm^3)	1.32	1.42	1.46	1.55	1.60	1.64	1.60	1.55
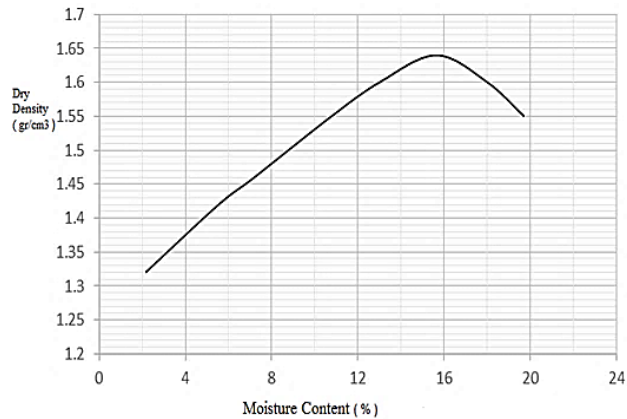
Figure 3. Clay compaction curve (C Method) (14)

Figure 4. Soil compaction test

2-3-2. Direct shear test (DIRECT SHEAR-ASTM D 3080-90)

Based on the results of direct shear tests and knowing the value of γ, the resistance parameters of clay soil, C and φ, can be achieved. After several impacts on the surface of the modeled soil within the test box and with the same compaction conditions, the hammer numbers were compared with the defined resistance parameters and verified (Moore, D.M, 1989).

2-4. Impact on the clay soil with a hammer test

After performing the compaction test and learning the maximum specific gravity, soil samples are molded in the moisture range of 0 to 15% in a sampling box measuring $15 \times 15 \times 15$ cm3 with a specific gravity of 1.18 g/cm3 and relative compaction of 71% to 95% in 17 laboratory parametric models. They are then examined by the rebound hammer impacts in horizontal and vertical directions as demonstrated in Figures (9) and (10). After concurrent recording, the read numbers undergo the direct shear test, and the results are compared with the hammer numbers. Ultimately, the definitive studies are performed and with only one of the presented parameters, the other parameters are properly estimated using correlation relationships and practical tables. Figures (5) to (10) show the steps of using the hammer (Keller, Thomas, M, 2014).
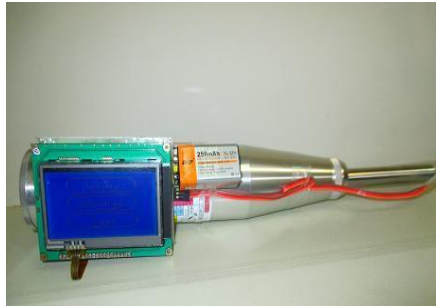
Figure 5. The test cube box

Figure 6. The rebound hammer

Figure 7. Steps of compressing the box

Figure 8. Impact test in the vertical direction

Figure 9. Impact test in the
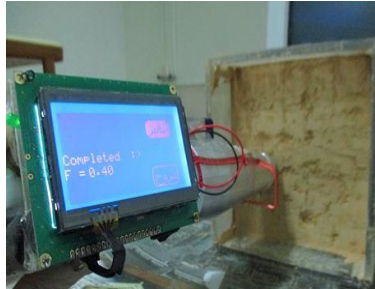horizontal direction

Figure 10. The box ready for the impact test

2-5. Quasi-dynamic analysis of the hammer impacts by MATLAB software

Checking the physical equations governing hammer before and after impact on the studied clay surfaces, and the amount of displacement, penetration depth, velocity, and acceleration obtained from the start to the end of the test, confirms the effect of shear waves due to physical work, and complete damping of the soil's spring-damper model system.

The hammer device holds a spring with a 30 N/m stiffness and a mass of 50 grams, with a structure similar to concrete Schmidt hammers. But its stiffness is 100 times smaller. The impact is transmitted to the electronic board by the force sensors. According to the programming done using the CodeVision software, the outputs are presented on the screen based on the stiffness and compaction percentage. The numbers read from the direct shear device and the compaction test are then calibrated in the laboratory. Next, the values of compaction percentage and stiffness of soil parametric samples are determined.

2-5-1. Physical equations of the device

The physical equations governing the reaction of hammer and soil, before impact and after the impact, are examined in this section.

2-5-1-1. Pre-impact hammer equations

Figure (11) displays the status of the hammer in three distinct modes. Table (2) also includes the characteristics of the physical parameters of the device. In mode 1, no pressure is imposed on the hammer and the inside spring is in a stationary state. If we mount the end rod of the hammer to the soil surface and impose pressure, the inside spring of the hammer is pulled, and ultimately, the device transits to mode 2. At the end of this mode, the hammer's latch is released and the

weight is dismissed. Then, the internal spring is immediately compressed, and the hammer goes to mode 3.

Table 2. Characteristics of the physical parameters of the rebound hammer device

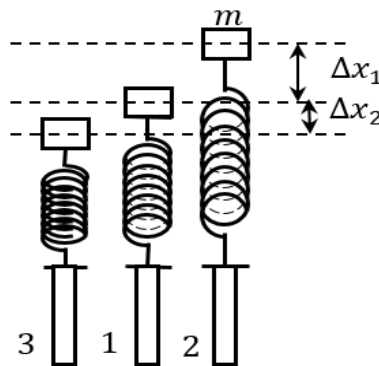| Parameter	Value
Spring stiffness	$30 \frac{N}{m}$
Mass weight	50 g
Maximum expansion	8 cm
Maximum contraction	4 cm

Figure 11. Three modes of the physical belongings of the hammer

By knowing the physical relationships, the device can provide the user with the values of energy, speed, acceleration, and pressure from the input impact in both horizontal and vertical directions. Figure (12) designates how the spring length changes owing to imposing force and releasing. In mode A, the spring has the most compaction and is then released. In mode B, the spring recovers to its original position, but since it has a velocity, it passes from this mode to mode C to undergo maximum expansion. The spring then returns to its original state in D from C, and because it has a velocity, it goes back to the maximum compaction state in E. This cycle is repeatable.
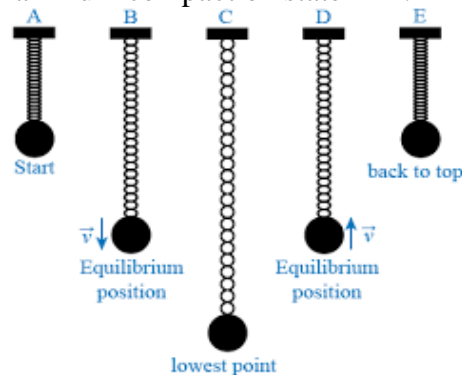

Figure 12. spring length changes due to imposing force and releasing

Differential equation governing the mass and spring system:

$$f = -kx \tag{1}$$

Further:

$$f = ma = m\ddot{x} \tag{2}$$

Therefore, by mixing (1) and (2) we have:

$$m\ddot{x} = -kx$$

$$m\ddot{x} + kx = 0$$

$$x = x.\cos\left(\sqrt{\frac{k}{m}}t\right)$$

Given that the spring is first compressed by 8 cm, we have x = 8 cm. Now we have according to the parameters of Table (2):

$$x = 0.08\cos\left(\sqrt{\frac{30}{0.05}}t\right) \cong 0.08\cos(24.5t)$$

And using the x equation, we can get the equation of velocity and acceleration:

$$v = \dot{x} = -1.96\sin(24.5t)$$
$$a = \ddot{x} = -48\cos(24.5t)$$

Now, using the x equation, we calculate the time of reaching the position x = -4 cm (moment of impact on the ground) in milliseconds:

$$-0.04 = 0.08\cos(24.5t) \rightarrow t_{impact} = 85.5\ ms$$

Now, using this time, we can calculate the velocity and acceleration at the moment of the impact:

$$v(t_{impact}) = -1.96\sin(24.5 \times 0.0855) \cong -1.69\ m/s$$
$$a(t_{impact}) = -48\cos(24.5 \times 0.0855) \cong 24\ m/s^2 \cong 2.45g$$

2-5-1-2. Post-impact hammer equations

The motion equation of the object after striking the soil is a second-order differential equation:

$$m\ddot{x} + c\dot{x} + kx = 0 \tag{3}$$

This equation is also represented as Equation (4):

$$\ddot{x} + 2\xi\omega_n\dot{x} + \omega_n{}^2 = 0 \tag{4}$$

Where ξ (Xi) damping ratio is a dimensionless quantity in physics that determines how an oscillating system is examined. For a harmonious oscillator with mass m and damping coefficient c and spring constant (stiffness) k, we have:

$$\xi = \frac{c}{cc} \tag{5}$$

Where critical damping coefficient is:

$$c_c = 2\sqrt{k.m} \tag{6}$$

Or:

$$c_c = 2m\omega_n \tag{7}$$

$$\omega_n = \sqrt{\frac{k}{m}} \tag{8}$$

Figure (13) shows the behavior of the soil for the damping ratio of $0 \le \xi$. As can be seen, for $\xi < 1$, the behavior is oscillating. According to the behavior of the second-order differential equation system (quasi-dynamic equation) and the perceived responses in soil oscillating behavior after the collision, and based on the results of MATLAB software analysis, soil's damping ratio is closer to 0.9. Thus, $\xi \cong 0.9$ (y(t): ξ = Damping coefficients) (Ogata, K, 2009).
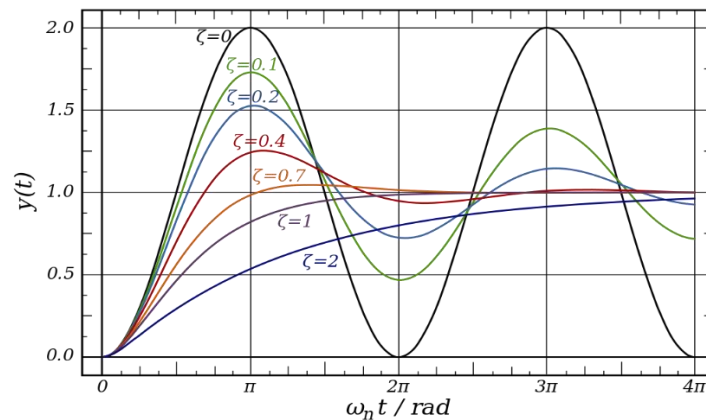

Figure 13. The behavior of the second-order differential system per different damping coefficient (Ogata, K, 2009)

2-5-2. Stiffness calculation

The stiffness of the parametric samples gathered from mathematical calculations with MATLAB software following the relation (9) and Figure (14) is determined in the quasi-dynamic equation

of the Viscoelastic spring-damper model following the hammer's impact on clay surface (Lin, J, 2014). Stiffness is achieved in non-damp K and damped Kd states.
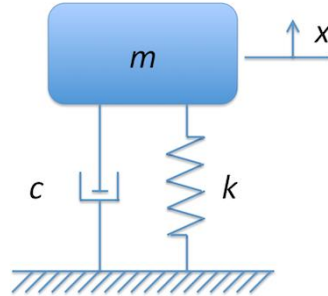
$$m\ddot{x} + c\dot{x} + kx = 0 \qquad (9)$$

Figure 14. Soil's spring-damper model

2-5-3. Penetration depth

To determine the penetration depth induced by the impact, we practice a recognized relationship (13):

$$DI = n\sqrt{W.H} \qquad (10)$$

Where n is a fixed number, and it is generally between 0 and 1. For the soil used in the examination, according to the existing references and experimentally, considering the engineering judgment, the value of n is considered to be between 0.3 and 0.4. H is the release height and W is the weight of the object released in tons. But in this research, the weight is not released but thrown. So the above relationship needs to adjust. Because in the normal release, only the gravity acceleration prompts impact to the ground, but in throwing, in addition to the acceleration of gravity, the acceleration obtained from the throw must likewise be regarded. According to earlier investigations, the acceleration gained from the launch at the moment of impact in the horizontal location is 2.45 g. Accordingly, the above relationship switches as follows:

$$DI_{new} = n\sqrt{2.45W.H} \qquad (11)$$

The weight of the projected weight is 50 grams and the projection height, according to Table (2) is:

$$H = 4 + 8 = 12 \; cm$$

Thus:

$$DI = 0.3\sqrt{2.45 \times 0.05 \times 10^{-3} \times 12 \times 10^{-2}} \cong 1.2 \; mm$$

As can be noticed, the penetration depth is 1.2 mm, which is in line with laboratory measurements.

2-5-3-1. The relationship between hammer penetration depth and the natural frequency of the system

According to Equation (12), we have:

$$\omega_n = \sqrt{\frac{k}{m}} \rightarrow fn = \frac{1}{2\pi}\sqrt{\frac{k}{m}} \tag{12}$$

On the other hand, based on (13), we have:

$$m = \frac{W}{g}. \quad x_s = \frac{W}{k}$$

Where W is the weight in Newton and x_s expresses the depth of penetration. Mixing the three equations leads us to:

$$\omega_n = \sqrt{\frac{k}{m}} = \sqrt{\frac{\frac{W}{x_s}}{\frac{W}{g}}} = \sqrt{\frac{g}{x_s}}$$

Heed that in this relation, the penetration depth xs is the same as DI in the preceding section.

The penetration depth is obtained from this equation and the control of laboratory notes. On the other hand, the natural frequency of the hammer system in damped oscillations (ω_d) can be determined from the natural frequency of the hammer system in undamped oscillations (ω_n) with a damping ratio of ξ = 0.9 according to Equation (14). Table (3) includes the corresponding results (13).

$$\omega_d = \sqrt{1 - \xi^2}\, \omega_n \tag{14}$$

3. RESULTS AND DISCUSSION

3-1. Natural frequencies of the system, stiffness, and wavelength

As Table (3) suggests, the frequency and stiffness drop because of the presence of a system dam due to the hammer impacts in the viscoelastic soil model examined.

Figures (2) to (7) demonstrate how the above variables change (Ostadan,F, et al. 2004), (Tahouni, Sh, 2011).

Table 3. Natural frequencies of the system, stiffness, and wavelength results

$\lambda\ (m)$	$k_d\ \left(\dfrac{N}{m}\right)$	$k\ \left(\dfrac{N}{m}\right)$	$\omega_d\ \left(\dfrac{rad}{s}\right)$	$\omega_n\ \left(\dfrac{rad}{s}\right)$	n	Sample No
0.132	60.705	319.504	34.844	79.938	0.400	1A
0.131	62.262	327.697	35.288	80.956	0.390	3A
0.130	63.071	331.953	35.516	81.480	0.385	4A
0.129	63.900	336.320	35.749	82.014	0.380	5A
0.128	65.100	342.632	36.083	82.780	0.373	2F
0.127	65.628	345.410	36.229	83.115	0.370	6A
0.126	67.451	355.005	36.729	84.262	0.360	5F
0.125	68.401	360.005	36.986	84.853	0.355	7A
0.124	69.378	365.148	37.250	85.457	0.350	9A
0.123	70.383	370.440	37.518	86.074	0.345	10A
0.122	71.418	375.888	37.793	86.705	0.340	9F
0.121	72.484	381.498	38.074	87.349	0.335	10F
0.119	74.485	392.030	38.596	88.547	0.326	12A
0.118	75.882	399.381	38.957	89.373	0.320	13A
0.117	77.086	405.720	39.264	90.080	0.315	14A
0.116	79.354	417.653	39.838	91.395	0.306	15A
0.115	80.941	426.006	40.234	92.304	0.300	16A

According to Table (3) and Figure (11), the maximum wavelength generated in the soil is after the collision and before damping.
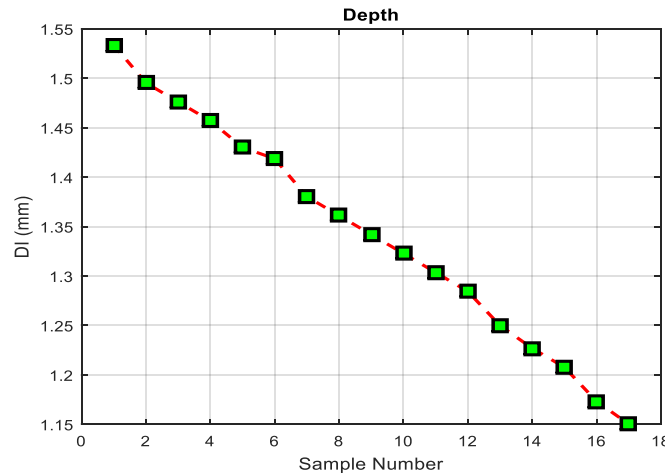

Figure 15. Depth of penetration changes in parametric models
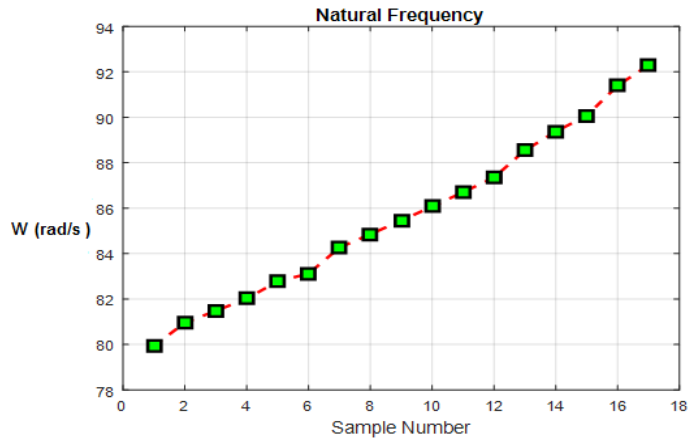
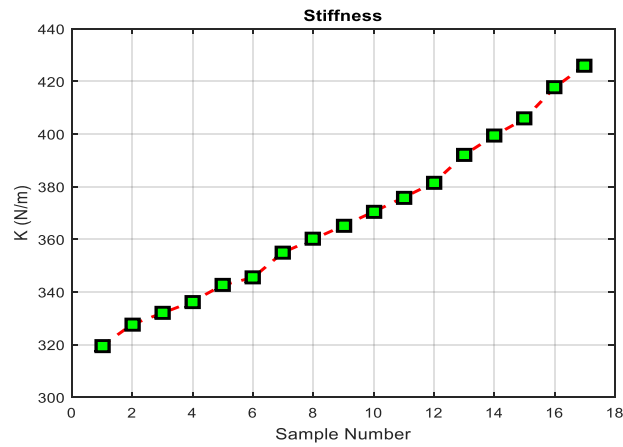Figure 16. Non-damped natural system frequency changes in parametric models

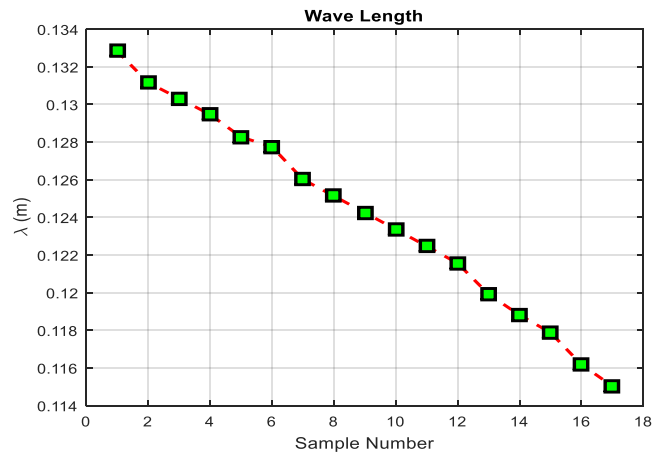Figure 17. Non-damped stiffness changes in parametric models

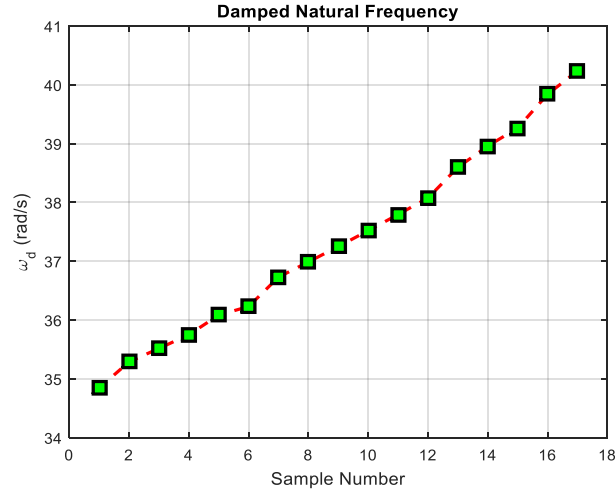Figure 18. Wavelength changes in parametric models

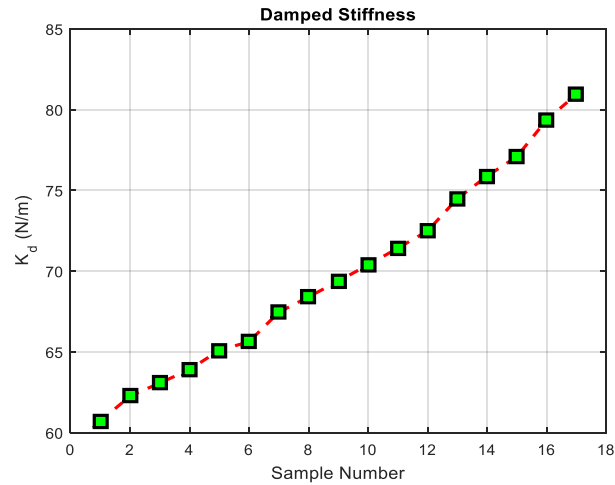Figure 19. The natural frequency of the damped system changes in parametric models

Figure 20. Damped stiffness changes in parametric models

3-2. Analysis of one of the parametric samples

To better perceive, the soil acceleration, velocity, and displacement changes Figures are plotted for one of the types of samples presented in the earlier part. According to the previous section, the stiffness coefficient of the latest soil sample is $k = 426\frac{N}{m}$. Thus, we have:

$$c = 2\xi\sqrt{k.m} = 2 \times 0.9 \times \sqrt{426 \times 0.05} \cong 8.3$$

And the ultimate equation of the soil is:

$$0.05\ddot{x} + 8.3\dot{x} + 426x = 0$$

Where x is the vertical or horizontal soil relocation. As we know, any second-order differential equation needs two initial conditions to solve. These initial conditions here are displacement (x_0)

726

and velocity ($\dot{x}_0 = v_0$). Provided that we take the initial soil level as the origin, we have x_0 = 0. On the other hand, according to the earlier section, if the hammer is employed in the vertical direction, the initial velocity of impact with the soil surface will be $\dot{x}_0 = v_0 = 1.69 \frac{m}{s}$. Consequently, with these initial conditions, the vertical displacement of the soil, velocity, and acceleration will be as in Figures (21) to (23).
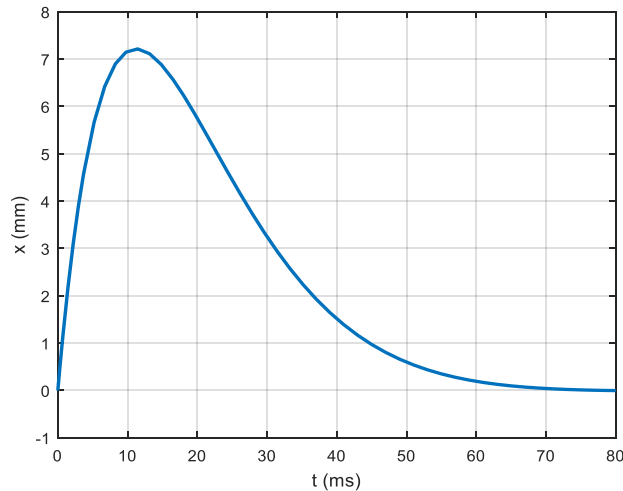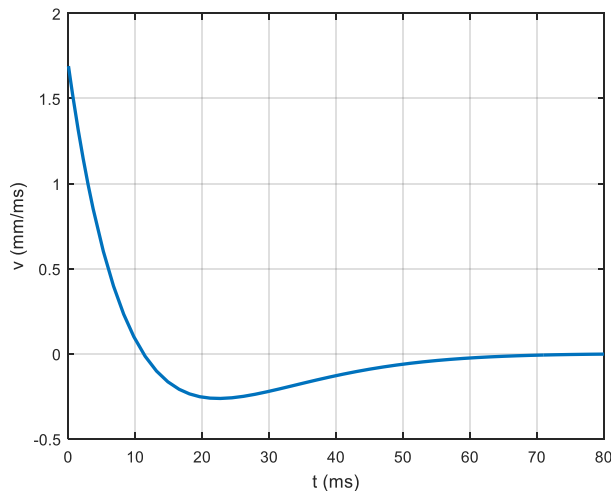

Figure 21. Vertical displacement of the soil in millimeters

(Figure 22) The vertical velocity of the soil

According to Figures 20 and 21, after the impact on the soil, it takes around 70 milliseconds for the conditions to recover to normal states and for the oscillations to damp. Furthermore, according to the Figure (20), nearly 12 milliseconds after the collision, the highest displacement occurs in the soil, by about 7 mm. Figure (23) further reveals the acceleration changes versus time.
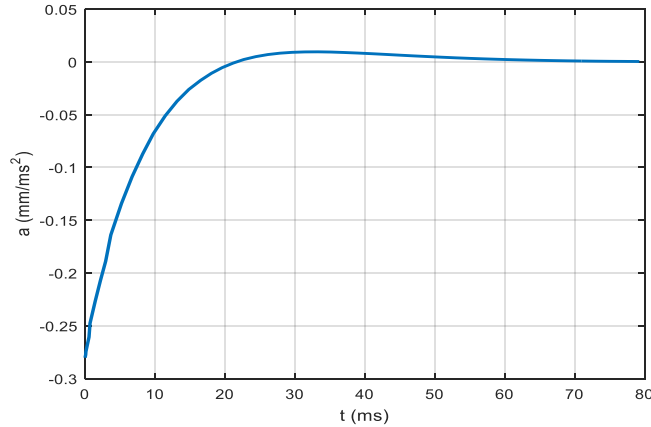
Figure 23. Acceleration versus time

3-2-1. Pre- and post-damping wavelength

Because of the characteristics of clay soils, the impact of waves disappears immediately within 0.8 seconds inside the soil mass. Accordingly, we must record and examine the mirrored information throughout the effective wavelength.

According to the acquired Figures from the numerical analysis of MATLAB software and laboratory controls, when the hammer hits the ground at the end of the mentioned period, the impact waves swiftly vanish. Consequently, it is essential to choose the dimensions of the soil sample cubic mold in the laboratory 15 * 15 * 15 cm3, so that the model bed would not harm the obtained results (12), (13).

3-3. Comparison of tested parameters

All parameters examined by correlation relationships and laboratory results are compared. The number N in the horizontal and vertical directions is the rebound number. This number is equivalent to the relative compaction and stiffness of the soil surface, been analyzed through correlation control tests and MATLAB software. In this regard, the effective behavioral parameters of the clay tested are usually incremental in terms of specific gravity and compaction, and N increases with compaction.
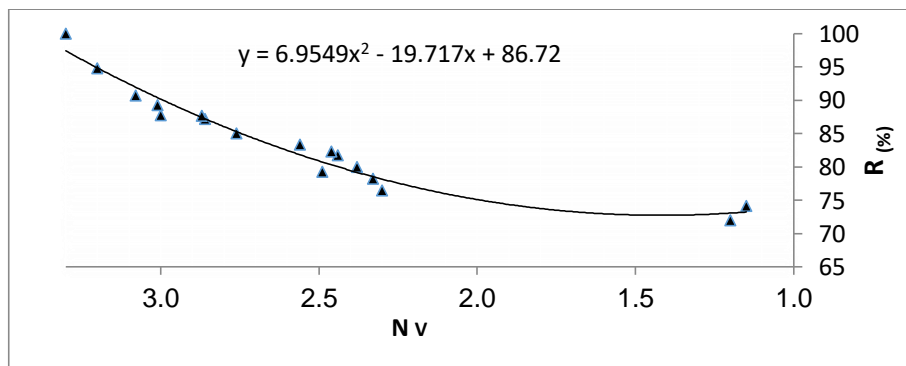

Figure 24. The relation between the soil compaction percentage with the vertical hammer reading
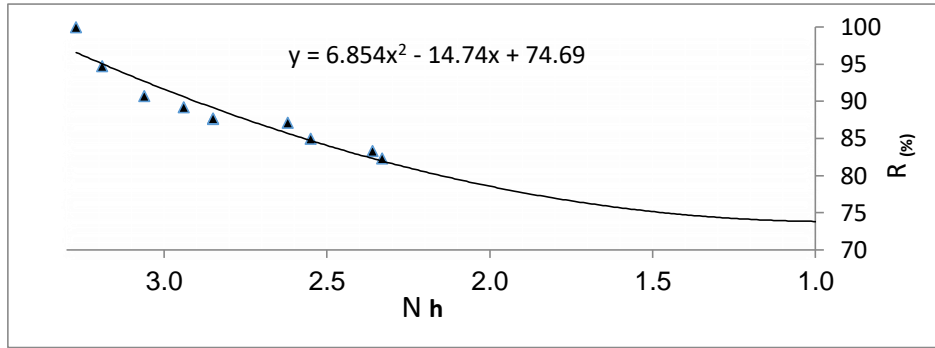
728

$$y = 6.854x^2 - 14.74x + 74.69$$

Figure 25. The relation between the soil compaction percentage with the horizontal hammer reading

Because of the frailty of the soil samples and their low compaction, the soil collapsed, and no numerical values were read. In higher figures, owing to the compaction of less than 82% and the moisture content of less than 2.2%, the number of hammers was presented in a low span and then moved upwards (Figure 25) and (Table 4).

$$y = 13.198x^3 - 66.442x^2 + 112.15x - 60.399$$
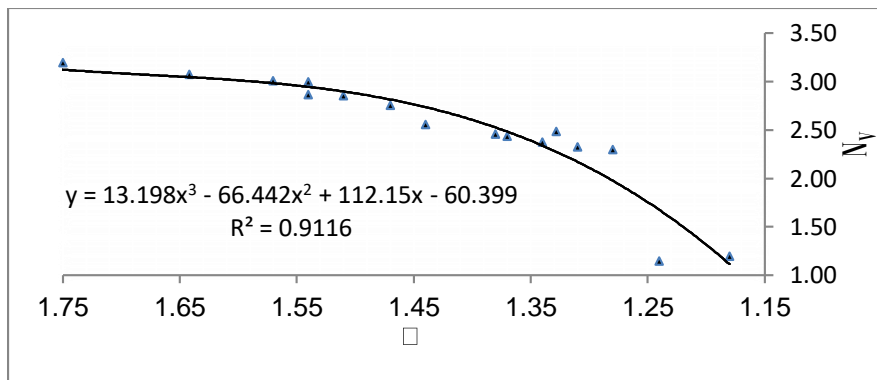$$R^2 = 0.9116$$

Figure 26. The relationship between the soil's specific gravity and vertical hammer numbers

All laboratory techniques were strictly monitored. According to the present Figures, increased and decreased compaction respectively increases and decreases the specific gravity. The results of the Figure (26) are gathered from the correlation equations.
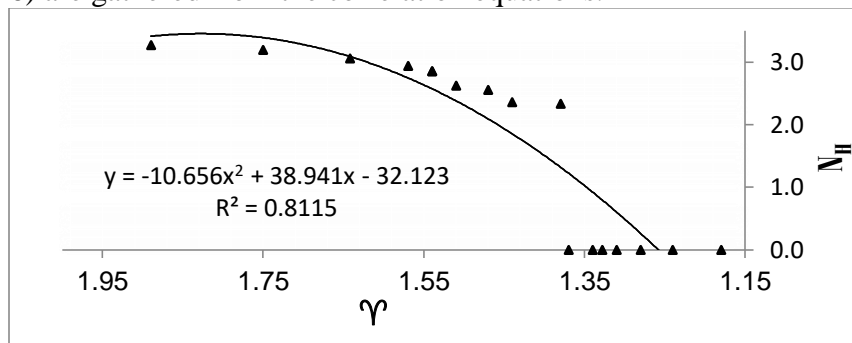

$$y = -10.656x^2 + 38.941x - 32.123$$
$$R^2 = 0.8115$$

Figure 27. The relationship between the soil's specific gravity and horizontal hammer numbers

729

In all in vitro experiments, the progressive increase in hammer numbers depended on the stiffness of the soil surface (Figure 27). The present study is a thorough laboratory work, confirmed by numerical analysis (MATLAB software). The relationship between dampened stiffness and specific gravity is displayed in Figures (28) and (29).
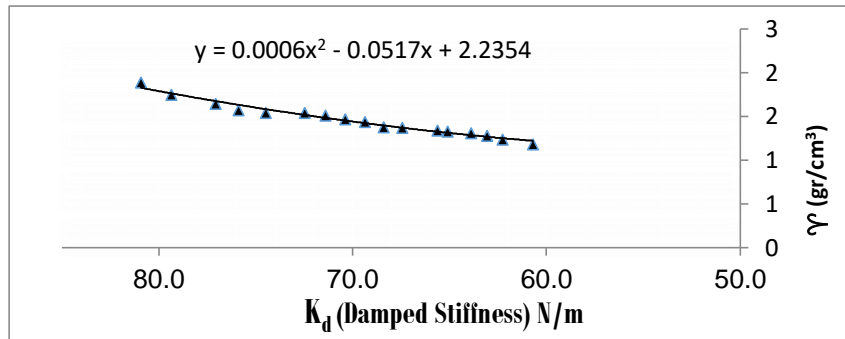

Figure 28. The relationship between the specific gravity and stiffness
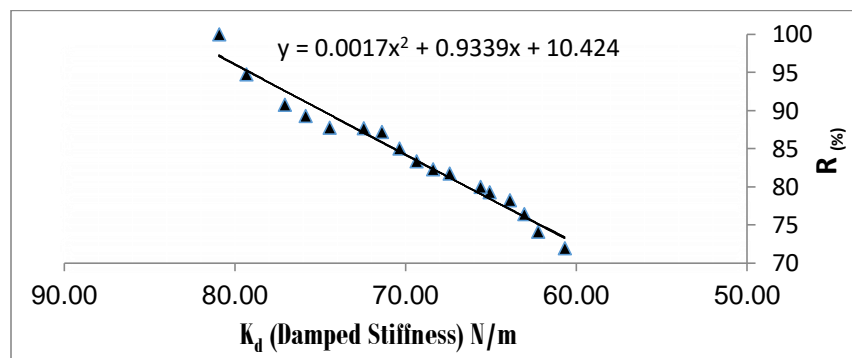

Figure 29. The relationship between the compaction percentage and stiffness

The results achieved from the in vitro methods and numerical control methods (MATLAB) on the 17 parametric examples of research obtained by the electronic hammer are listed in Table (4) (12). In Figure (29) and Table (4), soil stiffness increased with specific gravity and was controlled by the formula in Section 2-5-1-1.

Table 4. Concluding results of the research (in the range of 0 to 15% humidity)

Energy (N.m)	λ (m)	k_d (N/m)	ω_d (rad/s)	D_I (mm)	ε^p	n^*	ω (%)	N_h	N_v	R (%)	γ (gr/cm³)	Sample No
7.2e-5	0.132	60.705	34.844	1.54	0.090	0.400	0.00	(*)	1.20	71.95	1.18	1A
6.9e-5	0.131	62.262	35.288	1.49	0.126	0.390	1.97	(*)	1.15	74.14	1.24	3A
6.8e-5	0.130	63.071	35.516	1.47	0.106	0.385	2.04	(*)	2.30	76.46	1.28	4A
6.8e-5	0.129	63.900	35.749	1.46	0.104	0.380	2.09	(*)	2.33	78.23	1.31	5A
6.6e-5	0.128	65.100	36.083	1.43	0.120	0.373	2.11	(*)	2.49	79.27	1.328	2F
6.6e-5	0.127	65.628	36.229	1.42	0.113	0.370	2.13	(*)	2.38	80.0	1.34	6A
6.3e-5	0.126	67.451	36.729	1.37	0.135	0.360	2.18	(*)	2.44	81.71	1.37	5F
6.3e-5	0.125	68.401	36.986	1.36	0.096	0.355	2.20	2.33	2.46	82.32	1.38	7A
6.2e-5	0.124	69.378	37.250	1.34	0.155	0.350	5.32	2.36	2.56	83.35	1.44	9A
6.1e-5	0.123	70.383	37.518	1.32	0.100	0.345	5.43	2.55	2.76	85.0	1.47	10A
6.0e-5	0.122	71.418	37.793	1.30	0.163	0.340	5.57	2.62	2.86	87.19	1.51	9F
6.0e-5	0.121	72.484	38.074	1.29	0.170	0.335	7.10	2.85	2.87	87.68	1.54	10F
5.8e-5	0.119	74.485	38.596	1.25	0.161	0.326	7.00	2.85	3.00	87.74	1.54	12A

5.6e-5	0.118	75.882	38.957	1.22	0.141	0.320	7.20	2.94	3.01	89.26	1.57	13A
5.6e-5	0.117	77.086	39.264	1.21	0.162	0.315	10.28	3.06	3.08	90.73	1.642	14A
5.4e-5	0.116	79.354	39.838	1.17	0.131	0.306	12.57	3.19	3.20	94.75	1.750	15A
5.3e-5	0.115	80.941	40.234	1.15	0.156	0.300	15.00	3.27	3.30	100	1.89	16A

R(%) is the compaction percentage, (%) is the moisture percentage of the sample soil, Nv is the vertical hammer reading, Nh is the horizontal hammer reading, n* is the calibration coefficient of hammer penetration depth (based on dynamic soil compaction references and laboratory observations). Table (4) displays all the information gained from the in vitro tests performed and the previous Figures of parametric samples. The results are converged and corrected according to correlation relations and fitted mathematical equations. (*): Owing to the frailty of the samples and their low compaction, the soil collapsed, and no numbers were read.

4. CONCLUSIONS

Increased numbers (N) are directly correlated to the increased soil compaction and stiffness. Based on the definitive laboratory results, the hammer numbers above 3 in the vertical direction and 2.94 in the horizontal direction on clay surfaces, means 90% compaction, specific gravity above 1.34 gr/cm3, and higher soil stiffness (Table 4).

The ratio of hammer numbers in vertical and horizontal directions when they are closing together means compaction of higher than 90% of the soil.

It takes 70ms for the oscillations to happen after collision with the ground. Additionally, 12ms after the impact, the highest displacement occurs in the direction of the soil, by 7 mm (Figure 8).

Analyzing and determining the relationship between displacement, velocity, and acceleration due to hammer impact with compaction percentage, specific gravity, and stiffness of impermeable clay is decided by the results.

Compaction control conditions resulting by the hammer blower can be cited for soils following the materials of this study (kaolinite clay), with a moisture content of 0 to 15% and a maximum depth of 13 cm from the soil surface.

5. REFERENCES

Aflaki, I. (2008). Soil Mechanics Laboratory. University Press, Tehran, Iran.

Ashmawy, A. K., Rodrigo Salgado, Soumitra Guha, and V. P. Drnevich (1995). Soil damping and its use in dynamic analyses. International conferences on recent advances in geotechnical earthquake engineering and soil dynamics.

Dos, Brajaw, Translation, (2008). "Geotechnical Engineering Principles", Academic Edition, Fifth (in Persian) Edition, Iran, Tehran.

Eflaki, Ismail, (1989) "Soil Mechanics Laboratory", Amir Kabir University of Technology, Tehran,. (in Persian).

Hanumantha Rao, B., and Taradutta Panda. (2014) "A methodology for determining crushing strength of stabilized waste from shear wave velocity." International Journal of Geotechnical Engineering 8, no. 1: 84-93.

Iranian Schools' Renovation Organization, Concrete Technical Laboratory, and Soil Mechanics, Hamedan, Iran, (2016)

Keller, Thomas, M. Berli, S. Ruiz, Mathieu Lamandé, J. Arvidsson, Per Schjønning, and A. P. S. Selvadurai. (2014), "Transmission of vertical soil stress under agricultural tyres: Comparing measurements with simulations." Soil and Tillage Research 140 106-117.

Kramer, (2009) S. Seismic Geotechnical Engineering. Seyed Majeddin Mir Mohammad Hosseini. Tehran. Earthquake Research Institute.

Law, K.H. (2014) Determination of soil stiffness parameters at a deep excavation construction site in Kenny Hill Formation.

Lin, J., Y. Sun, and P. Schulze Lammers. (2014) Evaluating the model-based relationship of cone index, soil water content and bulk compaction using dual-sensor penetrometer data. Soil and Tillage Research. 138: 9-16.

Moore, D.M. and Reynolds Jr., (1989) R.CX-Ray Diffraction and the Identification and Analysis of Clay Minerals. Oxford University Press, Oxford, 179-20.

Naderi-Boldaji, Mojtaba, Reza Alimardani, Abbas Hemmat, Ahmad Sharifi, Alireza Keyhani, Mehari Z. Tekeste, and Thomas Kelle(2014)r. "3D finite element simulation of a single-tip horizontal penetrometer–soil interaction. Part II: Soil bin verification of the model in a clay-loam soil." Soil and Tillage Research 144: 211-219.

Ogata, K. (2009) Modern control engineering 5th edition. Lugar: Upper Saddle River, New Jersey 07458." ed: Prentice-Hall: p.55 and 169.

Ostadan, F., Nan Deng, and Roesset J.M. (2004) Estimating total system damping for soil-structure interaction systems. The Third UJNR Workshop is a Soil-Structure Interaction, Menlo Park, California.

Tahouni, Sh. (2011) Principles of Geotechnical Engineering (Volume 2). Pars Aein Publishing, Tehran.